RHEUMATOLOGY

Rheumatology 2010;49:246–258
doi:10.1093/rheumatology/kep357
Advance Access publication 9 December 2009

Original article

Age-related T-cell cytokine profile parallels corneal disease severity in Sjögren's syndrome-like keratoconjunctivitis sicca in CD25KO mice*

Cintia S. De Paiva[1], Cindy S. Hwang[1], John D. Pitcher III[1], Solherny B. Pangelinan[1], Ehsan Rahimy[1], Wei Chen[1,2], Kyung-Chul Yoon[3], William J. Farley[1], Jerry Y. Niederkorn[4], Michael E. Stern[5], De-Quan Li[1] and Stephen C. Pflugfelder[1]

Abstract

Objectives. IL-2rα $(CD25)^{-/-}$ mice develop autoimmunity and lymphoproliferative disorders, including SS-like disease. The objective of this study was to evaluate the severity of corneal epithelial disease and T-cell cytokine profile in the ocular surface tissues of CD25KO mice.

Methods. CD25KO mice were evaluated at 8, 12 and 16 weeks of age. Corneal epithelial smoothness and corneal permeability were measured. Phenotype of infiltrating lymphocytes was evaluated by immunohistochemistry. Th-1, -2 and -17 associated factors were measured by real-time PCR in cornea and conjunctiva and by Luminex immunobead assay in tears.

Results. Compared with 8-week-old wild-type (WT) mice, CD25KO mice of the same age had significantly greater corneal irregularity and a significant increase in the number of $CD4^+$ and $CD8^+$ T cells infiltrating the conjunctiva. CD25KO mice had significantly higher levels of IL-6, TGF-β1, IL-23R, IL-17A, IL-17F, IL-21, CCL20, IL-10, GATA-3 and IFN-γ mRNA transcripts in their cornea and conjunctiva than WT mice at 8 weeks. IL-17A and IL-17F mRNA transcripts peaked at 12 weeks, whereas IFN-γ spiked at 16 weeks in CD25KO mice. Increased expression of IL-17A and IL-17F at 12 weeks in CD25KO mice was accompanied by a worsening of corneal surface parameters and an increase of $CD4^+$ T cell infiltrating the cornea.

Conclusions. Disruption of IL-2 signalling in CD25KO mice results in age-dependent SS-like autoimmune lacrimal-keratoconjunctivitis. A mix of Th-1 and Th-17 cytokines was detected. The peak severity of corneal epithelial disease corresponded to the peak of IL-17 expression.

Key words: Sjögren's syndrome, Dry eye, $CD4^+$ T cell, IL-17, Th-17, Cytokines, IFN-γ.

BASIC SCIENCE

Introduction

SS is a systemic autoimmune disease that targets mucosal tissues and their supporting secretory glands. The eye and the mouth are its primary targets. SS has a reported prevalence of 0.15–3.3%, depending on the diagnostic criteria used [1–3]. Ninety-five percent of SS patients are women, typically peri- and post-menopausal, but patients as young as 20 years of age may also be affected. Primary SS develops in the absence of a defined CTD, whereas secondary SS occurs in patients with a defined CTD (most commonly RA) [4]. In patients with RA, the prevalence of KCS may be as high as 92% [5]. The cardinal manifestation of SS is dryness, resulting from exocrine gland dysfunction. The involved exocrine glands [including the lacrimal gland (LG)]

[1]Ocular Surface Center, Department of Ophthalmology, Cullen Eye Institute, Baylor College of Medicine, Houston, TX, USA, [2]School of Ophthalmology and Optometry, Eye Hospital, Wenzhou Medical College, Wenzhou, Zhejiang, China, [3]Department of Ophthalmology, Chonnam National University Medical School, Dong-Gu, Gwangju, South Korea, [4]Department of Opthalmology, University of Texas, Southwestern Medical Centre, Dallas, TX and [5]Department of Biological Sciences, Allergan Inc., Irvine, CA, USA.

Submitted 15 July 2009; revised version accepted 30 September 2009.

*Presented in part as abstract at the Annual Meeting of the Association for Research in Vision and Ophthalmology, from 27 April to 1 May 2008, Fort Lauderdale, FL, USA.

Correspondence to: Cintia S. De Paiva, Cullen Eye Institute, Baylor College of Medicine, 6565 Fannin Street, NC 205-Houston, TX 77030, USA. E-mail: cintiadp@bcm.tmc.edu

are infiltrated with lymphocytes, monocytes and plasma cells [6]. T-cell infiltration of the conjunctiva has been observed in both SS and non-SS KCS [7, 8]. Among dry-eye conditions, SS causes the most severe KCS (dye staining and goblet cell loss) and carries the greatest risk of developing sight-threatening corneal ulceration and perforation [9].

IL-2 is pleiotropic cytokine that has been identified to play a pivotal role in regulating the adaptive immune response [10]. Its multiple functions include stimulating proliferation of activated T cells ($CD4^-$, $CD8^-$, $CD4^-$, $CD8^+$, $CD4^+$ and $CD8^+$ lineages), proliferation and immunoglobulin synthesis by activated B cells, generation, proliferation and activation of NK cells and differentiation and maintenance of $FoxP3^+CD4^+CD25^+$ T regulatory cells (Tregs) [11–13]. IL-2 signals, through its heterotrimeric receptor, consists of α (IL-2rα, CD25), β (IL-2rβ, CD122) and γ (IL-2rγ, CD 132) chains. CD25KO mice have been recently proposed as an animal model of SS, since they spontaneously develop lymphocytic infiltration of their LG and salivary glands [14, 15]. These mice exhibit normal phenotype up to 4 weeks of age, after which they begin to show massive enlargement of lymph nodes, spleen and gut-associated lymphoid tissue due to polyclonal expansion of T and B cells [14, 15]. Fatal autoimmune complications ensue subsequently. Between 8 and 20 weeks, 25–50% of CD25KO-deficient mice die from severe haemolytic anaemia or fatal colitis.

Recently, IL-2 has been shown to down-regulate Th-17 differentiation [16], the newly identified Th lineage that has been linked to autoimmunity. IL-17A is the signature cytokine of the newly identified Th-17 pathway that has been implicated in autoimmunity in humans and also in animal models, such as experimental autoimmune encephalomyelitis (EAE), autoimmune uveitis (EAU), CIA and IBD [17–20]. IL-17A has been found to be elevated in psoriatic lesions [21, 22] in the SF of patients with RA [23], and vitreous of patients with uveitis [24, 25]. IL-17A expression was found in salivary gland ductal epithelial cells of SS patients and non-obese diabetic mice [26, 27]. We observed significantly higher Th-17--associated cytokine mRNA transcripts in the conjunctiva of dry-eye patients, including SS, compared with normal subjects. In our experimental dry-eye model, IL-17A was found to modulate the acute corneal barrier disruption that develops in response to desiccating stress [28].

The purpose of this study was to evaluate the effects of ageing on the severity of corneal epithelial disease and T-cell cytokine expression on the ocular surface of CD25KO mice.

Materials and methods

Animals

This research protocol was approved by the Baylor College of Medicine Center for Comparative Medicine, and it conformed to the standards in the ARVO Statement for the use of animals in Ophthalmic and Vision Research.

Heterozygous breeder pairs of $CD25^{+/-}$ mice in a C57BL/6 background (B6.129S4-*Il2ra*^{tm1Dw}/J) were purchased from Jackson Laboratories (Bar Harbor, ME, USA) for establishing breeder colonies. They were housed in our vivarium in a pathogen-free environment. The genotype of CD25KO mice was confirmed according to the Jackson Laboratories' protocol. Wild-type (WT) mice (C57BL/6) were purchased from Jackson Laboratories.

Mice were used at 8, 12 and 16 weeks of age. Seventy-two animals per time point (8, 12 and 16 weeks) per strain (CD25KO and WT) were used: 5 mice for histological sections, 15 for evaluation of corneal permeability, 32 for tear collection and 20 for gene analysis. Evaluation of corneal smoothness was performed immediately after the euthanasia, on the same mice that were used for evaluating gene expression.

Corneal permeability

Corneal epithelial permeability to Oregon green dextran [OGD; 70 000 molecular weight (MW); Invitrogen, Eugene, OR, USA] was assessed at each time point (8, 12 and 16 weeks) of both strains (CD25KO and WT, 10 eyes/group/experiment, in three different sets of experiments). Briefly, 0.5 μl of 50 μg/ml OGD was instilled onto the ocular surface 1 min before euthanasia. Corneas were rinsed with 2 ml of phosphate buffered saline (PBS) and photographed with a stereoscopic zoom microscope (model SMZ 1500; Nikon, Melville, NY, USA), under fluorescence excitation at 470 nm. The severity of corneal OGD staining was digitally graded as previously reported [29]. The mean fluorescence intensity measured inside the 2-mm central zone by the image analysis software (Metavue 6.2r; Molecular Devices, Sunnyvale, CA, USA) was transferred to a database and the results averaged within each group. Results are presented as mean (S.D.) of fluorescence grey levels.

Evaluation of corneal smoothness

Corneal smoothness was assessed in 40 eyes of each strain of mice, in four different sets of experiments [29]. Smoothness of images of a stereoscopic zoom microscope fibre optic ring illuminator (SMZ 1500; Nikon) reflected off the corneal surface was graded in digital images by two masked observers and averaged within each group. The corneal irregularity severity score was calculated using a 5-point scale based on the extent and severity of the distortion of the reflected ring, as previously described [29]. Results are presented as mean (S.D.)

Histology

Eyes and ocular adnexa, extraorbital LGs and submandibular salivary glands (SMGs) were surgically excised, fixed in 10% formalin, paraffin-embedded and sections of 8 μm were cut. Sections were stained with haematoxylin and eosin for the evaluation of morphology.

For immunohistochemistry, terminal deoxynucleotidyl transferase-mediated dUTP-nick end labelling (TUNEL) and IF assays, the eyes and adnexa of mice from each

strain/time point ($n = 5$) were excised, embedded in optimal cutting temperature compound (OCT compound; VWR, Suwanee, GA, USA) and flash frozen in liquid nitrogen. Sagittal 8-μm sections were cut with a cryostat (HM 500; Micron, Waldorf, Germany) and placed on glass slides that were stored at –80°C.

Tear peroxidase assay

Tear peroxidase activity was used as a measure of LG function [30]. Tear-fluid washings were collected from 20 animals/group, in two independent experiments, using a previously reported method [28]. One sample consisted of tear washings from both eyes of two mice pooled (4 μl) in PBS +0.1% BSA (6 μl) and stored at –80°C until the assay was performed. Tear peroxidase measurement was performed using an Amplex Red Peroxidase Kit, according to the manufacturer's instructions (Invitrogen-Molecular Probes, Eugene, OR, USA). There was a total of 10 samples from each strain per time point.

Immunohistochemistry

Immunohistochemistry was performed to detect and count the cells in the cornea, conjunctival epithelium and stroma that stained positively for CD4 (clone H129.9, 10 μg/ml, BD Bioscience, San Diego, CA, USA), CD8α (clone 53e6.7, 3.125 μg/ml, BD Bioscience), γδTCR (clone GL3,10 μg/ml, BD Bioscience), CD11b (clone M1/70, 6.25 μg/ml, monocytes/macrophages lineage, BD Bioscience), CD45 (bone marrow-derived cells, clone 30-F11, 10 μg/ml, BD Bioscience), CD11c (dendritic cells, clone HL3, 12.5 μg/ml, BD Bioscience), CD45RA (a marker of naïve T cells, clone 14.8, 10 μg/ml, BD Bioscience), CD103 (αE integrin, a marker of intra-epithelial lymphocytes, clone 2E7, 10 μg/ml, Biolegend, San Diego, CA, USA) and MPO (neutrophils, polyclonal sera, 1: 400; Fremont, NeoMarkers, Fremont, CA, USA).

Cryosections were stained with the aforementioned primary antibodies and appropriate biotinylated secondary antibodies (all from BD Pharmingen, San Diego, CA, USA) and a Vectastain Elite ABC kit using NovaRed reagents (Vector, Burlingame, CA, USA) as previously described [29]. Secondary antibody alone and appropriate anti-mouse isotype (BD Biosciences) controls were also performed. Three sections from each animal were examined and photographed with a microscope equipped with a digital camera (Eclipse E400 with a DS-Fi1; Nikon). Positively stained cells were counted in the goblet cell rich area of the conjunctiva, over a length of at least 500 μm in the epithelium and to a depth of 75 μm below the epithelial basement membrane in the stroma for a distance of 500 μm using image-analysis software (NIS Elements Software, version 3.0, BR; Nikon). Results were expressed as the number of positive cells per 100 μm. To determine the number of immune cells within the cornea, cells were counted over the entire segment of the cornea, from the superior to the inferior limbus, and the results are presented as the number of cells per cornea.

IF staining and laser scanning confocal microscopy

Cryosections stained for activated caspase 3 (1 : 100, 5 μg/ml, BD Pharmigen) were developed using goat anti-rabbit Alexa-Fluor 488 conjugated IgG antibody as previously described [29]. Negative controls were performed at the same time and consisted of sections incubated with an isotype antibody (BD Pharmigen) or sections with omitted primary antibody.

Digital images (512 × 512 pixels) of cryosections were captured with a laser-scanning confocal microscope (LSM 510; Zeiss with krypton–argon and He–Ne laser; Carl Zeiss Meditec, Ltd Thornwood, NY, USA) with 488- excitation and 543-nm emission filters, LP505 and LP560, respectively. They were acquired with a 40/1.3 × oil immersion objective.

TUNEL assay

The (TUNEL) assay was performed using a kit (ApopTag; Intergen Co., Purchase, NY, USA) [31]. Cryosections were fixed in 1% paraformaldehyde, and permeabilized with 2 : 1 ethanol: acetic acid solution. The samples were incubated with TdT enzyme and 11-digoxigenin dUTP at 37°C for 4 h. After quenching the reaction, samples were blocked with blocking solution and incubated with anti-digoxigenin FITC-conjugated antibody for 60 min at room temperature.

Multiplex cytokine immunobead assay

Tear washings were collected from 32 animals per group, in three independent experiments as previously reported [28]. One sample consisted of tear washings from both eyes of four mice pooled (8 μl) in mouse cytokine assay buffer (12 μl; Upstate-Millipore, Lake Placid, NY, USA) and stored at –80°C until the immunobead assay was performed. There was a total of eight samples from each strain per time point.

Tear washings (20 μl) were added to wells containing appropriate cytokine bead mixture that included mouse monoclonal antibodies specific for IL-1α, IL-1β, IL-6, IL-13, IFN-γ, IL-17, IL-12p40 and IL-12p70 (Upstate-Millipore). Since there are no commercially available beads to IL-23p19 (the exclusive subunit of IL-23), we evaluated the ratio of both subunits [IL-12p40 (the shared subunit between IL-23 and IL-12) and IL-12p70 (the exclusive subunit of IL-12)] as a measure of IL-23. Serial dilutions of the above cytokines were added to wells in the same plate as the mouse samples to generate a standard curve. The plates were incubated overnight at 4°C to capture the cytokines by the antibody conjugated fluorescent beads. After three washes with assay buffer, 25 μl of biotinylated secondary cytokine antibody mixture was applied for 1.5 h in the dark at room temperature. The reactions were detected with streptavidin–phycoerythrin using a Luminex 100 IS 2.3 system (Austin, TX, USA).

RNA isolation and real-time PCR

Total RNA from the cornea and conjunctiva (individually collected and individually pooled) from CD25KO and WT mice at each time point (8, 12 and 16 weeks)

was extracted using an acid guanidium thiocyanate–phenol–chloroform method as previously described [29]. Four samples per strain were used, and one sample consisted of pooled samples from five mice per time point. Samples were treated with DNase to prevent genomic DNA contamination according to the manufacturer's instructions (Qiagen, Valencia, CA, USA).

First-strand cDNA was synthesized from 1 μg of total RNA using random hexamers and M-MuLV reverse transcriptase (Ready-To-Go You-Prime First-Strand Beads; GE Healthcare, Piscataway, NJ, USA), as previously described [29]. Real-time PCR was performed using gene expression assay primers and MGB probes specific for murine *GAPDH, IL-6, IL-23, TGF-β1, IL-17A, IL-23 receptor, IL-17 receptor, RORγt, STAT3, IL-21, IL-22, CCL20, IL-17F, IFN-γ, IL-2, IL-12, T-bet, IL-4, IL-13, GATA-3, STAT3, STAT5 and IL-10* (Assay IDs: Mm99999915, Mm00446490, Mm00518984, Mm00441724 17241, Mm00439619, Mm00519942, Mm00434214, Mm00441139, Mm00456961, Mm00517640, Mm00444 4241, Mm00444228, Mm00521423, Mm00801778, Mm00434256, Mm00434165, Mm00450960, Mm00445 259, Mm00434204, Mm00484683, Mm00839861 and Mm00439616, respectively). The GAPDH gene was used as an endogenous reference for each reaction. The results of quantitative PCR were analysed by the comparative C_T method where target change $= 2^{-\Delta\Delta Ct}$ (User Bulletin, No. 2, P/N 4303859; ABI, Foster City, CA, USA). The cycle threshold (C_T) was determined using the primary (fluorescent) signal as the cycle at which the signal crossed a user-defined threshold. The results were normalized by the C_T value of GAPDH and the mean C_T of relative mRNA level in the C57BL/6 group at 8 weeks of age was used as the calibrator.

Statistical analysis

One-way analysis of variance (ANOVA) with Tukey's *post hoc* testing was used for statistical comparisons of tear cytokines and gene expression in profiles of cornea and conjunctiva within strains. Two-way ANOVA with Tukey's *post hoc* testing was used for statistical comparison between strains. The normality of data was checked with the Kolmogorov–Smirnov test using the Dallal and Wilkinson approximation. Both tear cytokines and gene expression profiles passed this normality test. $P \leqslant 0.05$ was considered statistically significant. These tests were performed using GraphPad Prism 5.0 software (GraphPad Software Incorporation, San Diego, CA, USA).

Results

CD25KO mice develop lymphocytic infiltration of LG and salivary glands, cornea and conjunctiva

We compared the LG and SMGs and ocular surface tissues of CD25KO mice at 8, 12 and 16 weeks of age with age-matched WT C57BL/6 mice (Fig. 1). As previously reported [32, 33], we observed that CD25KO

Fig. 1 Representative images of haemotoxylin and eosin-stained LG and SMG sections of aged C57BL/6 WT and CD25KO mice (from 8 to 16 weeks). Normal LG morphology was noted in the C57BL/6 WT at all time points, in contrast to CD25KO LG, which showed lymphocytic infiltration (circumscribed by black dotted lines) at all time points. The last images on the right are higher magnification of area demarcated by white dotted square in LG of both strains. In the CD25KO SMG sections, periductal infiltration was noted as early as 8 weeks (black dotted lines) and acinar atrophy was present at 16 weeks of age.

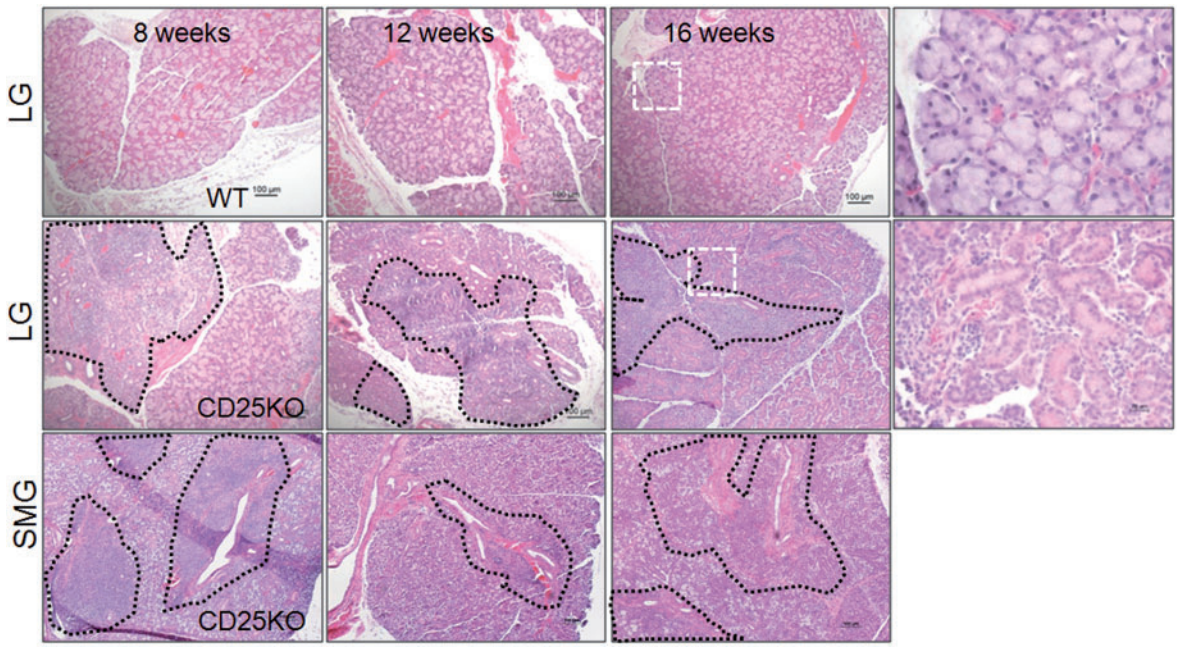

mice develop spontaneous lymphocytic infiltration of these exocrine glands. Macroscopically, the extra-orbital LGs were enlarged and inflamed at 8 and 12 weeks, but they were significantly smaller at 16 weeks, compared with WT LG. Microscopically, we noted lymphocytic infiltration occupying ~50% of the LG at all ages evaluated in CD25KO mice. This infiltration was noted as early as 8 weeks of age. At 16 weeks, much of the LG was atrophic and also showed periductal fibrosis, enlargement of the epithelial ducts and abnormally appearing acini. The LG pathology was further investigated and reported in a separate study (Rahimy *et al*., submitted). The lacrimal immunopathology was accompanied by secretory dysfunction. Peroxidase content in tears was only measurable in WT mice [3.23 (2.07), 2.77 (2.12), 2.55 (1.40) Horseradish Peroxidase (HRP) mUmol, respectively, for 8, 12 and 16 weeks of age], whereas it was below the detection level at all ages in the CD25KO mice (all <1.5 HRP mUmol).

We observed a similar pattern of lymphocytic infiltration in the CD25KO SMG, which showed intense periductal lymphocytic infiltration at 8 weeks of age that progressed to enlargement of ducts and gland disorganization with ageing.

The conjunctiva of 8-week-old CD25KO mice also exhibited a significant $CD4^+$ (Fig. 2C and H) and $CD8^+$ (Table 1); T-cell infiltration was compared with WT mice of the same age. The maximal $CD4^+$ infiltration in the cornea and conjunctiva was found at 12 weeks (Table 1). We observed $CD4^+$ T cells in the mid-peripheral and central cornea of CD25KO mice, areas that are normally devoid of T cells in WT mice (data not shown). The phenotype of infiltrating cells in the conjunctiva and cornea is presented in Table 1.

CD25KO mice spontaneously develop KCS and epithelial apoptosis

We then investigated if increased lymphocytic infiltration of ocular surface tissues in CD25KO mice would correspond to corneal epithelial pathology. Our results are presented in Fig. 2. We observed that young, 8-week-old CD25KO mice had decreased corneal surface smoothness (Fig. 2A and F) compared with 8-week-old WT. Ageing further decreased the corneal regularity and worsened the corneal barrier function measured by OGD staining (Fig. 2B and G) at 12 weeks of age in CD25KO mice. Activated caspase 3 staining was negative in the WT mice at all time points, whereas intense cytoplasmic expression was noted in the corneal and conjunctival epithelium of CD25KO mice. The expression of activated caspase 3 progressively worsened with ageing, and it was maximal at 16 weeks in the CD25KO mice (Fig. 2D).

Fig. 2 Ocular surface evaluation of aged C57BL/6 and CD25KO mice from 8 to 16 weeks of age: corneal smoothness (**A**), corneal permeability to OGD (**B**) and conjunctival $CD4^+$ T-cell immunostaining (in red, **C**)**.** Merged images of laser-scanning IF confocal microscopy of cornea and conjunctiva sections stained for activated caspase 3 (in green, D) or processed for TUNEL assay (green, **E)** with propidium iodide nuclear counterstaining (in red). Orange colour in TUNEL indicates co-localization of green and red nuclear staining. Mean (S.D.) of corneal smoothness score (**F**)**,** OGD staining score (**G**) and $CD4^+$ T-cell density in the conjunctival epithelium (**H**). IL-17/IFN-γ mRNA ratio in corneal epithelial mRNA transcripts. Conj: conjunctiva; 8W: 8 weeks; 12W: 12 weeks; 16W: 16 weeks. $^*P < 0.05$ *vs* C57BL/6 or CD25KO at 8 weeks of age; $^{**}P < 0.001$ *vs* C57BL/6 or CD25KO at 8 weeks of age.

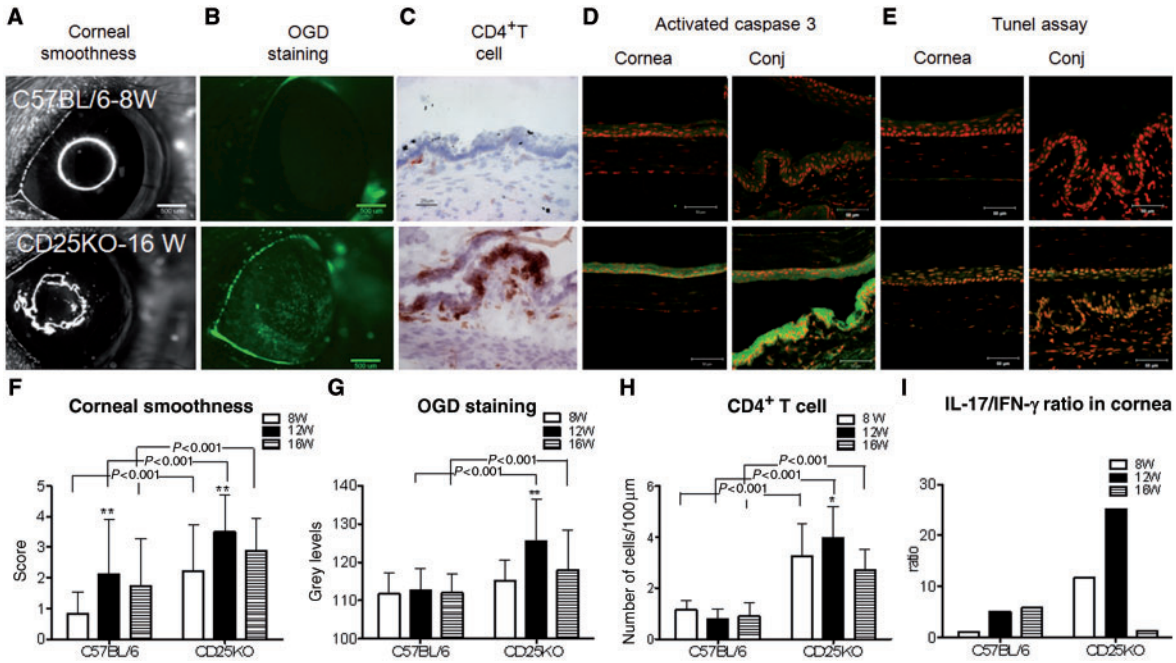

Table. 1 Summary of immune cell populations detected by immunostaining in the conjunctiva (CJ) and cornea of C57BL/6 WT and CD25KO mice at different ages

Mouse strain	8W	12W	16W	*P*-value strains
CD4 (cornea)				
C57BL/6	5.18 (2.95)	2.00 (2.24)	2.67 (2.91)	<0.001 at 12W
CD25KO	4.50 (4.79)	12.44 (5.73)**	4.29 (3.99)	
CD8 (cornea)				
C57BL/6	2.30 (3.07)	4.00 (2.91)	1.48 (2.91)	>0.05
CD25KO	2.78 (2.49)	5.90 (4.07)	2.00 (0.71)	
CD4 CJ				
E				
C57BL/6	1.31 (0.43)	0.75 (0.40)	0.90 (0.53)	<0.001 at 8W and 16W
CD25KO	3.81 (1.25)	3.39 (0.72)*	2.69 (0.99)	<0.05 at 12W
S				
C57BL/6	3.40 (1.53)	1.07 (0.72)***	1.21 (0.76)***	<0.001 at 12W
CD25KO	3.84 (0.46)	4.08 (2.12)*	3.20 (1.23)	
CD8 CJ				
E				
C57BL/6	0.95 (0.35)	0.59 (0.40)	1.00 (0.41)	<0.001 at 8W, 12W, 16W
CD25KO	4.20 (1.25)	3.48 (1.20)	3.64 (0.99)	
S				
C57BL/6	0.48 (0.32)	0.78 (0.62)	1.10 (0.62)***	<0.001 at 8W, 12W <0.05 at 16W
CD25KO	3.12 (0.88)	3.34 (2.27)	3.05 (1.26)	
CD11b CJ				
E				
C57BL/6	1.61 (0.85)	1.90 (1.17)	2.47 (1.44)	<0.01 at 8W
CD25KO	3.51 (1.54)	3.28 (1.19)	2.60 (0.98)	<0.05 at 12W
S				
C57BL/6	7.23 (1.70)	2.01 (0.92)***	2.52 (0.84)***	<0.001 at 8W
CD25KO	3.65 (1.76)	2.88 (1.13)	2.26 (1.28)	
CD45 CJ				
E				
C57BL/6	4.17 (1.48)	4.22 (1.20)	5.49 (1.56)	<0.01 at 8W
CD25KO	7.88 (2.97)	7.01 (2.25)	6.36 (1.97)	<0.05 at 12W
S				
C57BL/6	6.06 (1.97)	6.03 (1.83)	7.11 (2.25)	>0.05
CD25KO	5.54 (1.37)	5.81 (1.82)	6.29 (1.20)	
CD11c CJ				
E				
C57BL/6	0.40 (0.52)	0.64 (0.30)	1.14 (0.61)*	>0.05
CD25KO	1.06 (0.33)	1.40 (0.90)	1.27 (0.56)	
S				
C57BL/6	0.25 (0.24)	0.86 (0.40)***	0.55 (0.08)*	<0.01 at 8W
CD25KO	0.22 (0.08)	0.33 (0.21)	0.28 (0.11)	<0.05 at 12W
CD103 CJ				
E				
C57BL/6	0.82 (0.28)	0.52 (0.20)	0.59 (0.38)	<0.01 at 12W
CD25KO	1.14 (0.58)	1.69 (1.22)	0.89 (0.37)	
S				
C57BL/6	0.30 (0.22)	0.32 (0.13)	0.33 (0.10)	>0.05
CD25KO	0.48 (0.26)	0.43 (0.27)	0.41 (0.31)	
CD45RA CJ				
E				
C57BL/6	0.36 (0.39)	0.42 (0.13)	0.58 (0.12)	<0.001 at 12W
CD25KO	1.11 (0.56)	1.77 (0.61)*	1.44 (1.09)	
S				
C57BL/6	0.06 (0.08)	0.79 (0.44)***	0.53 (0.42)	<0.001 at 12W
CD25KO	0.18 (0.06)	0.22 (0.07)	0.31 (0.14)	
Myelo CJ				
E				
C57BL/6	0.88 (0.63)	0.65 (0.29)	0.53 (0.20)	<0.05 at 16W
CD25KO	0.66 (0.43)	1.21 (0.99)	1.59 (0.90)*	
S				
C57BL/6	1.02 (0.58)	0.65 (0.55)	0.73 (0.48)	<0.01 at 8W
CD25KO	0.33 (0.15)	0.42 (0.35)	0.38 (0.38)	

Asterisks indicate within-strain comparison. The *P*-values between strain comparisons are shown at the left column. Data presented as mean (S.D.) (cells/100 μm) for the conjunctiva and number of cells per cornea for the cornea. CJ: conjunctiva; E: epithelium; S: stroma; Myelo: MPO; $^{*}P < 0.05$ within the same strain; $^{**}P < 0.01$, $^{***}P < 0.001$ within the same strain compared with 8 weeks. 8W: 8 weeks; 12W: 12 weeks; 16W: 16 weeks.

TUNEL assay confirmed the results of activated caspase 3 IF staining: TUNEL positive (+) cells were observed in corneal and conjunctival epithelia of CD25KO mice, whereas they were rarely observed in WT mice (Fig. 2E). Ageing further worsened apoptosis: at 8 weeks, TUNEL+ cells were noted throughout the basal layer of cornea and conjunctival epithelium, whereas at 16 weeks, TUNEL+ cells were found in all cell layers (basal, subapical and apical) in the CD25KO mice.

These findings indicate that CD25KO mice spontaneously exhibit KCS (corneal irregularity, barrier dysfunction and epithelial apoptosis) at similar levels of severity to those observed in C57BL/6 WT mice that were subjected to experimental desiccating stress [29, 31]. The increased number of infiltrating T cells in cornea and conjunctiva prompted us to investigate the T cell-associated profile of cytokines using real-time PCR.

Inflammatory cytokines are present in tears

We measured an array of inflammatory/immune cytokines (IL-1α, IL-1β, IL-6, IL-12p40, IL-12p70, IL-17, IL-13 and IFN-γ) in tears of CD25KO and WT mice at all time points. Assays were performed on three independent sets of tears to confirm their reproducibility. The measured concentrations of these cytokines are shown in Fig. 3. At 8 weeks, CD25KO mice exhibited significantly higher levels of IL-1α and IFN-γ and a non-significant trend towards increased concentrations of IL-6, IL-1β, IL-12p40 and IL-17 in their tears compared with WT mice.

CD25KO mice showed a shift in Th-associated cytokine profile with ageing

Levels of significant changes in mRNA transcripts for Th-1, -2 and -17-associated factors/cytokines in the

Fig. 3 Cytokine concentrations measured in tear fluid of C57BL/6 WT and CD25KO mice at different ages, using Luminex multiplex immunobead assay. Data are mean (S.D.) (error bars) for three separate experiments. Dotted lines indicate the lowest value in the linear portion of the curve, generated from the observed mean fluorescent intensities *vs* the observed concentrations of standards. *$P < 0.05$ when compared with C57BL/6 at 8 weeks of age.

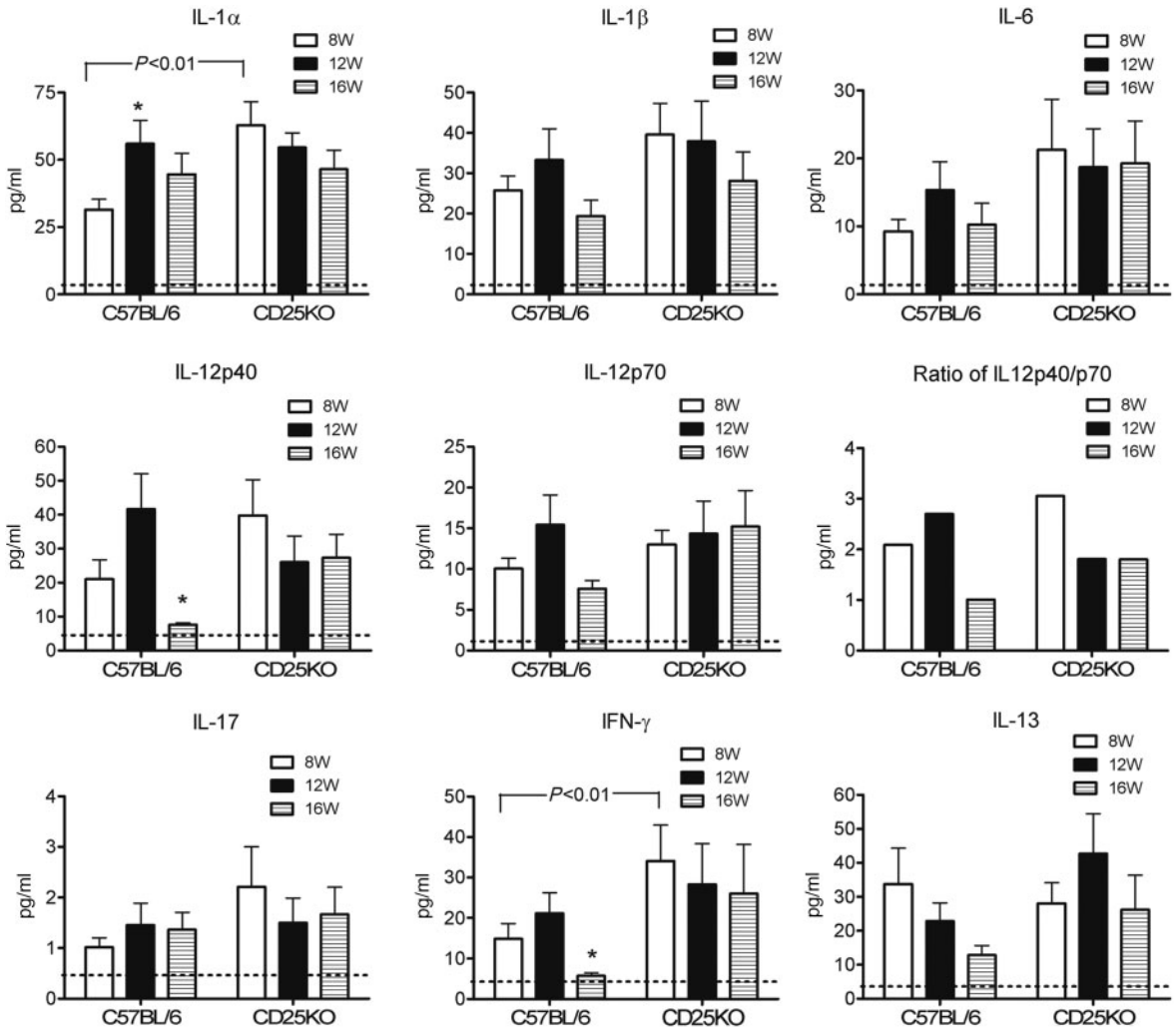

conjunctiva and cornea are presented in Figs 4 and 5, respectively.

Young (8-week-old) CD25KO mice had significantly higher levels of *IL-6, TGF-β1, IL-23R, IL-17A, IL-17F, IL-21, CCL20, IL-10, GATA-3* and *IFN-γ mRNA* transcripts in their conjunctiva than similarly aged *C57BL/6* control mice. Age-specific cytokine expression patterns were observed. At 12 weeks of age, *CD25KO* mice maintained high levels of *IL-6* and *IFN-γ* in the conjunctiva. They also had a significant increase in *IL-17A, IL-17F* and *IL-21 mRNA* transcripts. Interestingly, at 16 weeks of age, expression of *IL-17* effector genes (*IL-17A, IL-17F, IL-21* and *CCL20*) decreased, whereas up-regulation of other genes (*IL-23R, IL-17R, GATA-3*) was observed. TGF-β1 mRNA levels dropped at 12 weeks, but showed an enormous peak at 16 weeks (12-fold). IFN-γ mRNA transcript levels also significantly increased at 16 weeks (9.5-fold). It is worth noting that levels of the immunoregulatory cytokine *IL-10* showed a continuous decrease with ageing. These changes were not observed in the WT conjunctiva. No change was observed in levels of *MMP-9, IL-23, RORγT, STAT3, IL-12, T-bet, STAT5 and IL-13* transcripts between the two strains and within each strain with ageing (data not shown).

The pattern of gene expression in the *CD25KO* corneal epithelium was similar to the conjunctiva. Levels of Th-17-associated factors/cytokines (*IL-6, IL-17A, IL-17F* and *IL-21*) peaked at 12 weeks, whereas TGF-β1 peaked at 16 weeks of age. Young *CD25KO* mice showed significantly higher T-bet and IL-10 mRNA transcripts than WT mice, but a decrease in both factors was noted with ageing. No change was observed in levels of *MMP-9, TGF-β2, IL-12, IL-13, IL-15, CCL20, IL-23R, RORγT, STAT3* and *STAT5* transcripts between the two strains (data not shown). A non-significant increase in expression of *IFN-γ* was noted with ageing in the *CD25KO* mice (data not shown).

IL-4 mRNA transcripts were not detected in the WT cornea and conjunctiva at any time points. There was no change in the levels of *IL-22* and *IL-4* in the cornea and conjunctiva of *CD25KO* mice with ageing (data not shown).

Because of the distinct pattern of expression of *IL-17* and *IFN-γ*, signature cytokines of *Th-17* and *Th-1* pathways, respectively, we calculated the ratio of *IL-17/IFN-γ* to determine the predominant Th pathway at each age. Our results, presented in Fig. 2I, show greater *IL-17/IFN-γ* ratio in the cornea of 12-week-old CD25KO mice (a ratio of 25.24, compared with a ratio of 5.06 in 12-week-old WT), a finding that coincided with the greatest observed derangement of corneal barrier function, greatest corneal surface irregularity and T-cell infiltration of the cornea and conjunctiva during the observation period.

Discussion

CD25KO mice have been noted to develop spontaneous lymphocytic infiltration of multiple organs, such as bone marrow, colon, lung, pancreas and exocrine glands (including LG and SMG) [33]. The ocular surface of these mice has not been investigated in detail. In the present study, we demonstrated that CD25KO mice spontaneously exhibited SS-like features, including T-cell infiltration of the exocrine glands (LG and SMG) and ocular surface tissues (conjunctiva and cornea), a decrease of LG function, an increased corneal irregularity and barrier derangement, increased epithelial apoptosis and increased concentrations of inflammatory cytokines in tears. We also observed age-related changes in T-cell gene expression profile in the cornea and conjunctiva epithelia. These findings were equal to or greater than those observed in C57BL/6 mice subjected to desiccating stress [28, 29], demonstrating that CD25KO mice are a valid animal model of SS.

CD25KO mice are phenotypically similar to IL-$2^{-/-}$ mice. Both mice exhibit early autoimmunity and early mortality, primarily due to autoimmune haemolytic anaemia and colitis [14, 15]. IL-2 is a potent pleiotropic cytokine on the immune function. There are several hypotheses why CD25KO mice develop lymphocytic proliferation and autoimmunity. First, IL-2 controls the size of peripheral lymphoid compartment, by stimulating T cells to undergo activated cell death [14]. This mechanism has been implicated in limiting the number of autoreactive T cells that can participate in autoimmune reactions [15]. Secondly, CD25KO mice have defective $CD4^+$ $CD25^+$ Tregs, which compromise their ability to control self-reactive T cells. IL-2KO and CD25KO mice lack natural Tregs.

Spontaneous lymphocytic infiltration was observed in the LG and SMG of IL-2KO and CD25KO mice, but not in mice lacking Fox $P3^+$ cells (scurfy mice) [32]. However, neonatal scurfy mice can be induced to develop salivary gland inflammation if they are treated orally with LPS, a potent Toll-like receptor (TLR) agonist [32]. These results suggest that another mechanism, in addition to defects in Treg activity, may be implicated in autoimmunity and inflammation in the IL-2- and CD25-deficient mice.

Another hypothesis is the ability of IL-2 to function as a negative regulator of the Th-17 pathway. Genetic deletion or antibody blockade of IL-2 promoted differentiation of the Th-17+ cells [16]. Th-17 is a newly identified Th pathway, implicated in the pathogenesis of several human autoimmune diseases, including psoriasis, RA and in animal models of multiple sclerosis (EAE) and dry eye [17–20, 23, 28]. Elevated levels of IL-17A protein were recently found elevated in minor salivary glands of SS patients compared with normal subject controls [34]. IL-17A has a pathogenic role in dry eye; neutralization of IL-17 ameliorated desiccating stress-induced corneal barrier dysfunction [28]. The findings in our study also point to a pathogenic role of IL-17A in corneal disease. We observed that CD25KO mice spontaneously developed corneal barrier dysfunction at 12 weeks of age and this was accompanied by increased IL-17 expression and an increased IL-17/IFN-γ ratio in the corneal epithelium.

We found a significant increase of TGF-β mRNA in cornea and conjunctiva epithelia of CD25KO mice at

Fig. 4 mRNA transcript levels of Th-17 inducers (**A**), Th-17 (**B**), Th-1 and Th-2 (**C**) pathways in aged conjunctiva of C57BL/6 and CD25KO mice (8, 12 and 16 weeks of age). Data are shown as the mean (S.E.M.) ($n = 4$/time point, $^{*}P < 0.05$, $^{**}P < 0.01$, $^{***}P < 0.001$ *vs* 8 W within the same strain, compared with 8 weeks; 8W: 8 weeks; 12W: 12 weeks; 16W: 16 weeks; ND: non-detectable.

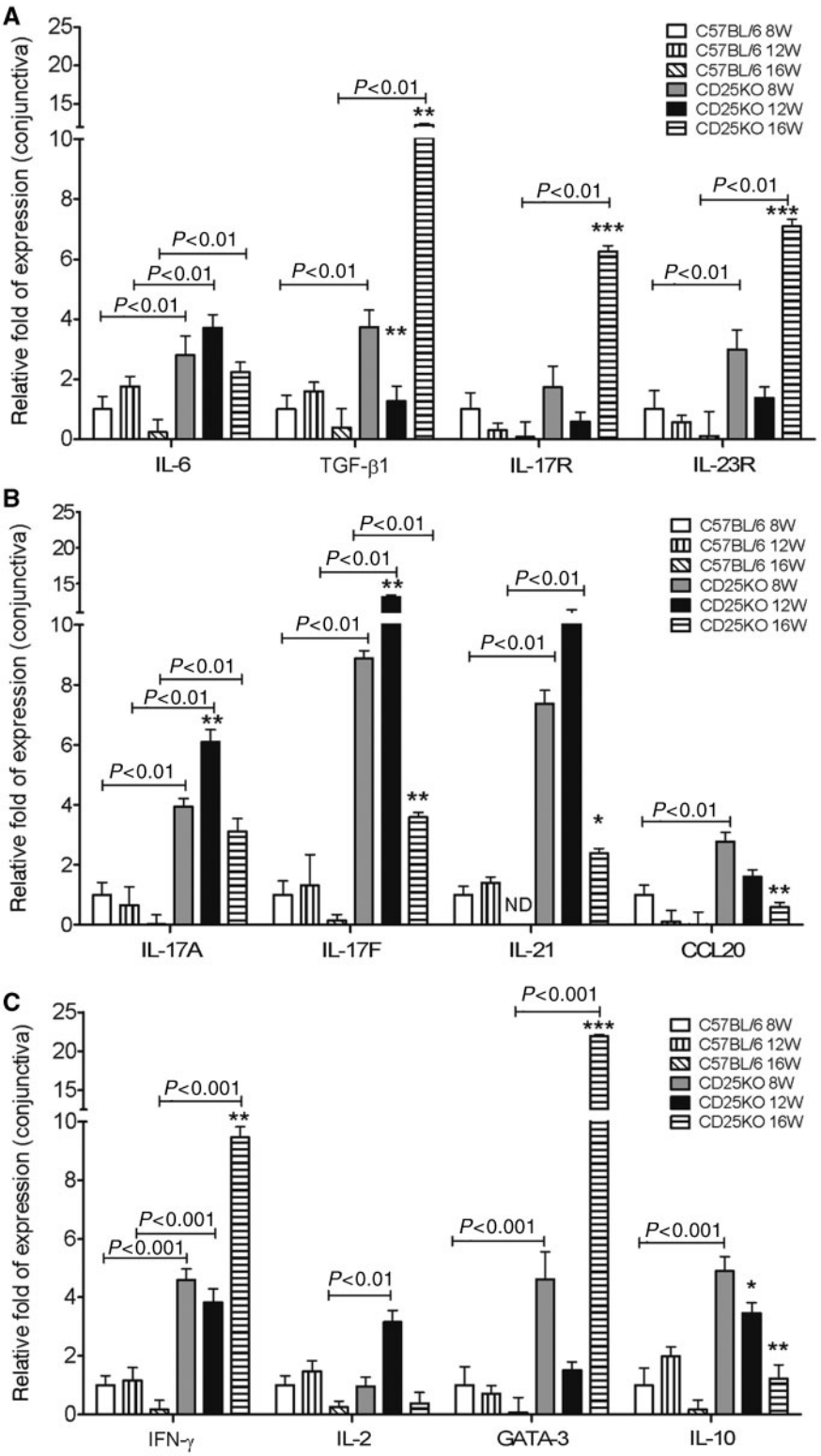

Fig. 5 mRNA transcript levels in corneal epithelia of Th-17 inducers (**A**), Th-17 (**B**), Th-1 and Th-2 (**C**) pathways in aged C57BL/6 and CD25KO mice (8, 12 and 16 weeks of age). Data are shown as the mean (S.E.M.) ($n = 4$/time point, $^{*}P < 0.05$, $^{**}P < 0.01$, $^{***}P < 0.001$ *vs* 8W within the same strain, compared with 8 weeks; 8W: 8 weeks; 12W: 12 weeks; 16W: 16 weeks; ND: non-detectable.

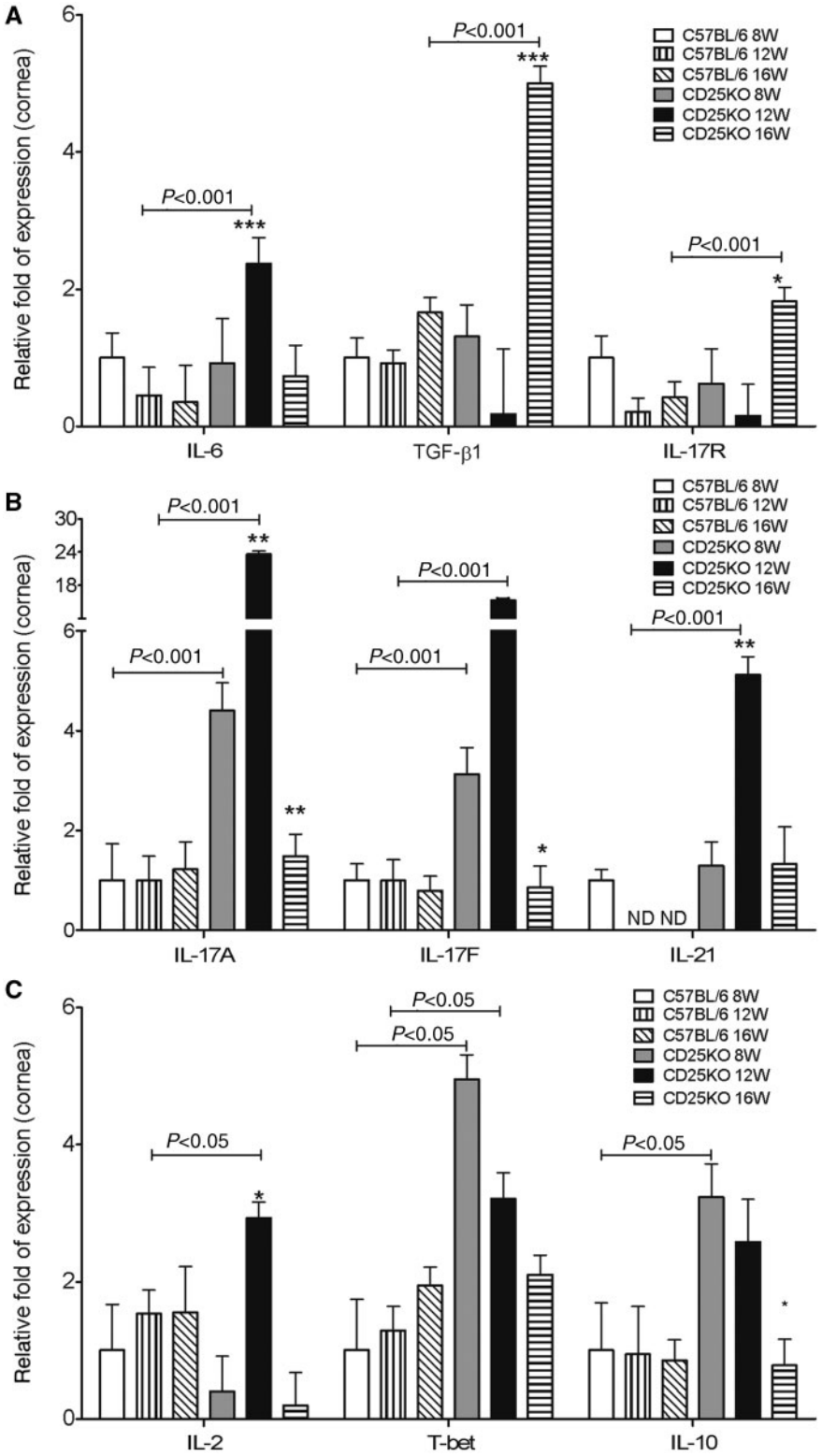

16 weeks of age. TGF-β is a multifunctional cytokine that has multiple functions: to inhibit or stimulate cell growth, regulate the immune system and enhance the synthesis and deposition of extracellular matrix during wound repair [35]. TGF-β has been detected in human tears, LG and conjunctival goblet cells [36–38]. Levels of mRNA transcripts, encoding several inflammatory cytokines (including TNF-α, IL-1α and -β, IL-6, IL-8, IL-10 and TGF-β1), were found to be elevated within the conjunctival epithelium of SS patients compared with non-dry-eye controls [39, 40]. These findings were recently confirmed in an experimental model of dry eye, where significantly higher TGF-β1 mRNA transcripts and protein levels were found in the cornea and conjunctiva epithelia of these mice [28]. TGF-β1, IL-6 and IL-23 expression was also found elevated in human biopsies of SS patients, with a concomitant increase in IL-17 protein expression compared with normal control subjects [34]. These findings are relevant because TGF-β has been shown to convert naïve CD4 cells into Foxp-3+ cells *in vitro* [41]. However, addition of IL-6 to the cultures promoted a decrease of Foxp3 and a concomitant increase of IL-17 mRNA transcripts. It has also been shown that TGF-β synergizes with IL-6 to induce the expression of the transcription factor RORγt, a key regulator of Th-17 differentiation [41–44]. The pro-inflammatory cytokine milieu may, therefore, drive the differentiation of naïve $CD4^+$ T cells into Th-17 or Tregs. At this point, we are not clear about the effects of the increased TGF-β1 expression on the autoimmune reaction on the CD25KO model. Nevertheless, as CD25KO mice lack $CD4^+CD25^+$ Tregs, promoting Treg differentiation would not be an effect of TGF-β1 in this model. Ageing could increase the mucosal exposure to microorganisms and environmental antigens than could activate TLR pathways and trigger auto-immunity, similar to that seen in scurfy mice treated with LPS [32]. The myeloid differentiation factor 88 (MyD88) is a key adaptor molecule required for signal transduction through TLRs. It has been shown that in animal models which use complete Freund's adjuvant (CFA), such as EAE and adoptive transfer colitis, $MyD88^{-/-}$ mice exhibited blunted disease and decreased production of IL-17 [45–47]. CFA contains pathogen-associated molecular patterns that bind TLR, and it has been used for *years* to boost immune responses in these models. In support of these findings, we have recently demonstrated that supernatant of human-cultured corneal epithelial cells treated with TLR agonists was capable of inducing IL-17-producing cells [34].

We also noted an increase of Th-1-associated cytokines, including IFN-γ in tears and mRNA transcripts in the cornea and conjunctiva of aged CD25KO mice. Several lines of evidence, such as high levels of serum IFN-γ and high levels of IFN-γ mRNA in conjunctiva of SS patients, indicate that IFN-γ is associated with the pathogenesis of SS [28, 48]. Treatment with IFN-γ induced the expression of HLA-DR, CD80 and ICAM on cultured salivary gland epithelial cells from SS patients [49]. Expression of high levels of IFN-γ mRNA in labial salivary gland biopsies from SS patients correlated with degree of T-cell infiltration [50]. Interestingly, knocking-out IFN-γ and IFN-γ receptor genes in the autoimmune-prone NOD mouse strain (which also develops spontaneous autoimmune exocrinopathy) reversed the lymphocytic infiltration of the submandibular glands and improved the secretory function of the salivary gland. However, NOD/IFN-γKO and NOD/IFN-γ receptor knock out (KO) mice still developed dacryoadenitis [51]. In an experimental model of dry eye, IFN-γKO mice were noted to develop corneal barrier disruption, but were resistant to goblet cell loss in response to experimental desiccating stress [28, 52]. Thus, neither IFN-γ nor IL-17 alone accounts for the full spectrum of pathological processes that produce dry-eye disease.

It is possible that in CD25KO mice the Th-1 and Th-17 pathways act synergistically to induce autoimmunity. In experimental models of IBD, both IFN-γ andIL-17A were found to synergize in triggering severe intestinal inflammation [53, 54]. In EAU, neutralization of IL-17A prevented or reversed disease in the absence of IFN-γ, following immunization with the retinal antigen interphotoreceptor retinoid-binding protein (IRBP) in CFA. However, induction of EAU using IRBP-pulsed mature dendritic cells required the generation of IFN-γ, as an IL-17A response by itself was insufficient to elicit pathology [25, 55]. In the CNS, it has been proposed that Th-17 cells may constitute the first wave of T cells migrating to the CNS and they may coordinate the recruitment of subsequent waves of effector T cells, particularly Th-1 cells, by secreting chemokines such as MCP-1 and IP-10 [56]. Specific vaccination strategies against infection with *Mycobacterium tuberculosis* have shown that the elicitation of an early Th17 response is essential in promoting a sustained Th-1 response that ultimately controls the pathogen [54].

In conclusion, disruption of IL-2 signalling in CD25KO mice results in age-dependent SS-like autoimmune lacrimal-keratoconjunctivitis. A mix of Th-1 and Th-17 cytokines was detected, with an early predominance of IL-17 and a late dominance of IFN-γ. The peak severity of corneal epithelial disease corresponded to the peak of IL-17 expression. These results suggest that both Th-1 and Th-17 cells are required for the full expression of dry eye disease, and thus are potential therapeutic targets for managing this potentially blinding disease.

Rheumatology key messages

- Ageing induces specific changes in lacrimal-keratoconjunctivitis in CD25KO mice, with a mix of Th-1 and Th-17 cytokines.
- The peak severity of corneal epithelial disease corresponded to the peak of IL-17 expression.

Acknowledgement

Funding: This work was supported by the National Institutes of Health Grants EY11915 to S.C.P.; Fight for Sight Grants-in-aid to C.S.D.P.; Hartford Foundation

to C.S.D.P.; Research to Prevent Blindness, Oshman Foundation; William Stamps Farish Fund; Hamill Foundation and an unrestricted grant from Allergan Inc. The sponsor agencies had no involvement in the study design; data collection, analysis and interpretation of data; in the writing of the report; or in the decision to submit the paper for publication.

Disclosure statement: M.E.S. is an employee of Allergan, Inc. All other authors declare no conflict of interest.

References

1 Andrianakos A, Trontzas P, Christoyannis F *et al*. Prevalence of rheumatic diseases in Greece: a cross-sectional population based epidemiological study. The ESORDIG Study. J Rheumatol 2003;30:1589–601.

2 Zhang NZ, Shi CS, Yao QP *et al*. Prevalence of primary Sjogren's syndrome in China. J Rheumatol 1995;22: 659–61.

3 Thomas E, Hay EM, Hajeer A, Silman AJ. Sjogren's syndrome: a community-based study of prevalence and impact. Br J Rheumatol 1998;37:1069–76.

4 Pflugfelder SC, Whitcher J, Daniels T. Sjögren's syndrome. In: Pepose JS, Holland GN, Wilhelmus KR, eds Ocular infection and immunity. St Louis: Mosby, 1996:1043–7.

5 Fujita M, Igarashi T, Kurai T, Sakane M, Yoshino S, Takahashi H. Correlation between dry eye and rheumatoid arthritis activity. Am J Ophthalmol 2005;140:808–13.

6 Carsons S. A review and update of Sjogren's syndrome: manifestations, diagnosis, and treatment. Am J Manag Care 2001;7:S433–43.

7 Pflugfelder SC, Huang AJW, Schuchovski PT, Pereira IC, Tseng SCG. Conjunctival cytological features of primary Sjogren syndrome. Ophthalmology 1990;97:985–91.

8 Raphael M, Bellefqih S, Piette JC, Le HP, Debre P, Chomette G. Conjunctival biopsy in Sjogren's syndrome: correlations between histological and immunohistochemical features. Histopathology 1988;13:191–202.

9 Pflugfelder SC, Tseng SCG, Sanabria O *et al*. Evaluation of subjective assessments and objective diagnostic tests for diagnosing tear-film disorders known to cause ocular irritation. Cornea 1998;17:38–56.

10 Waldmann TA. The biology of interleukin-2 and interleukin-15: implications for cancer therapy and vaccine design. Nat Rev Immunol 2006;6:595–601.

11 Waldmann TA, Dubois S, Tagaya Y. Contrasting roles of IL-2 and IL-15 in the life and death of lymphocytes: implications for immunotherapy. Immunity 2001;14: 105–10.

12 Miyazaki T, Liu ZJ, Kawahara A *et al*. Three distinct IL-2 signaling pathways mediated by bcl-2, c-myc, and lck cooperate in hematopoietic cell proliferation. Cell 1995;81: 223–31.

13 Fontenot JD, Rasmussen JP, Gavin MA, Rudensky AY. A function for interleukin 2 in Foxp3-expressing regulatory T cells. Nat Immunol 2005;6:1142–51.

14 Sadlack B, Merz H, Schorle H, Schimpl A, Feller AC, Horak I. Ulcerative colitis-like disease in mice with a disrupted interleukin-2 gene. Cell 1993;75:253–61.

15 Willerford DM, Chen J, Ferry JA, Davidson L, Ma A, Alt FW. Interleukin-2 receptor alpha chain regulates the size and content of the peripheral lymphoid compartment. Immunity 1995;3:521–30.

16 Laurence A, Tato CM, Davidson TS *et al*. Interleukin-2 signaling via STAT5 constrains T helper 17 cell generation. Immunity 2007;26:371–81.

17 Komiyama Y, Nakae S, Matsuki T *et al*. IL-17 plays an important role in the development of experimental autoimmune encephalomyelitis. J Immunol 2006;177: 566–73.

18 Nakae S, Komiyama Y, Nambu A *et al*. Antigen-specific T cell sensitization is impaired in IL-17-deficient mice, causing suppression of allergic cellular and humoral responses. Immunity 2002;17:375–87.

19 Nakae S, Nambu A, Sudo K, Iwakura Y. Suppression of immune induction of collagen-induced arthritis in IL-17-deficient mice. J Immunol 2003;171:6173–7.

20 Park H, Li Z, Yang XO *et al*. A distinct lineage of CD4 T cells regulates tissue inflammation by producing interleukin 17. Nat Immunol 2005;6:1133–41.

21 Haider AS, Lowes MA, Suarez-Farinas M *et al*. Identification of cellular pathways of ''type 1,'' Th17 T cells, and TNF- and inducible nitric oxide synthase-producing dendritic cells in autoimmune inflammation through pharmacogenomic study of cyclosporine A in psoriasis. J Immunol 2008;180:1913–20.

22 Zaba LC, Cardinale I, Gilleaudeau P *et al*. Amelioration of epidermal hyperplasia by TNF inhibition is associated with reduced Th17 responses. J Exp Med 2007;204: 3183–94.

23 Hwang SY, Kim HY. Expression of IL-17 homologs and their receptors in the synovial cells of rheumatoid arthritis patients. Mol Cells 2005;19:180–4.

24 Chi W, Zhu X, Yang P *et al*. Upregulated IL-23 and IL-17 in Behcet patients with active uveitis. Invest Ophthalmol Vis Sci 2008;49:3058–64.

25 Luger D, Silver PB, Tang J *et al*. Either a Th17 or a Th1 effector response can drive autoimmunity: conditions of disease induction affect dominant effector category. J Exp Med 2008;205:799–810.

26 Nguyen CQ, Hu MH, Li Y, Stewart C, Peck AB. Salivary gland tissue expression of interleukin-23 and interleukin-17 in Sjogren's syndrome: findings in humans and mice. Arthritis Rheum 2008;58:734–43.

27 Sakai A, Sugawara Y, Kuroishi T, Sasano T, Sugawara S. Identification of IL-18 and Th17 cells in salivary glands of patients with Sjogren's syndrome, and amplification of IL-17-mediated secretion of inflammatory cytokines from salivary gland cells by IL-18. J Immunol 2008;181: 2898–906.

28 de Paiva CS, Chotikavanich S, Pangelinan SB *et al*. IL-17 disrupts corneal barrier following desiccating stress. Mucosal Immunology 2009;2:243–53.

29 de Paiva CS, Corrales RM, Villarreal AL *et al*. Apical corneal barrier disruption in experimental murine dry eye is abrogated by methylprednisolone and doxycycline. Invest Ophthalmol Vis Sci 2006;47:2847–56.

30 Marcozzi G, Liberati V, Madia F, Centofanti M, de Feo G. Age- and gender-related differences in human lacrimal fluid peroxidase activity. Ophthalmologica 2003;217: 294–7.

31 Yeh S, Song XJ, Farley W, Li DQ, Stern ME, Pflugfelder SC. Apoptosis of ocular surface cells in experimentally induced dry eye. Invest Ophthalmol Vis Sci 2003;44:124–9.

32 Sharma R, Zheng L, Guo X, Fu SM, Ju ST, Jarjour WN. Novel animal models for Sjogren's syndrome: expression and transfer of salivary gland dysfunction from regulatory T cell-deficient mice. J Autoimmun 2006;27:289–96.

33 Sharma R, Bagavant H, Jarjour WN, Sung SS, Ju ST. The role of Fas in the immune system biology of IL-2R alpha knockout mice: interplay among regulatory T cells, inflammation, hemopoiesis, and apoptosis. J Immunol 2005;175:1965–73.

34 Katsifis GE, Rekka S, Moutsopoulos NM, Pillemer S, Wahl SM. Systemic and local interleukin-17 and linked cytokines associated with Sjogren's syndrome immunopathogenesis. Am J Pathol 2009;175:1167–77.

35 Lawrence DA. Transforming growth factor-β: a general review. Eur Cytokine Netw 1996;7:363–74.

36 Gupta A, Monroy D, Ji Z, Yoshino K, Huang AJW, Pflugfelder SC. Transforming growth factor beta-1 and beta-2 in human tear fluid. Curr Eye Res 1996;15:605–14.

37 Yoshino K, Garg R, Monroy D, Ji Z, Pflugfelder SC. Production and secretion of transforming growth factor beta (TGF-β) by the human lacrimal gland. Curr Eye Res 1996;15:615–24.

38 Pflugfelder SC, de Paiva CS, Villarreal AL, Stern ME. Effects of sequential artificial tear and cyclosporine emulsion therapy on conjunctival goblet cell density and transforming growth factor-beta2 production. Cornea 2008;27:64–9.

39 Jones DT, Monroy D, Ji Z, Pflugfelder SC. Alterations of ocular surface gene expression in Sjogren's syndrome. Adv Exp Med Biol 1998;438:533–6.

40 Pflugfelder SC, Jones D, Ji Z, Afonso A, Monroy D. Altered cytokine balance in the tear fluid and conjunctiva of patients with Sjogren's syndrome keratoconjunctivitis sicca. Curr Eye Res 1999;19:201–11.

41 Bettelli E, Carrier Y, Gao W *et al*. Reciprocal developmental pathways for the generation of pathogenic effector TH17 and regulatory T cells. Nature 2006;441:235–8.

42 Veldhoen M, Hocking RJ, Atkins CJ, Locksley RM, Stockinger B. TGFbeta in the context of an inflammatory cytokine milieu supports de novo differentiation of IL-17-producing T cells. Immunity 2006;24:179–89.

43 Mangan PR, Harrington LE, O'Quinn DB *et al*. Transforming growth factor-beta induces development of the T(H)17 lineage. Nature 2006;441:231–4.

44 Ivanov II, McKenzie BS, Zhou L *et al*. The orphan nuclear receptor RORgammat directs the differentiation program of proinflammatory IL-17+ T helper cells. Cell 2006;126:1121–33.

45 Fukata M, Breglio K, Chen A *et al*. The myeloid differentiation factor 88 (MyD88) is required for CD4+ T cell effector function in a murine model of inflammatory bowel disease. J Immunol 2008;180:1886–94.

46 Tomita T, Kanai T, Fujii T *et al*. MyD88-dependent pathway in T cells directly modulates the expansion of colitogenic CD4+ T cells in chronic colitis. J Immunol 2008;180:5291–9.

47 Marta M, Meier UC, Lobell A. Regulation of autoimmune encephalomyelitis by toll-like receptors. Autoimmun Rev 2009;8:506–9.

48 Konno A, Takada K, Saegusa J, Takiguchi M. Presence of B7-2+ dendritic cells and expression of Th1 cytokines in the early development of sialodacryoadenitis in the IqI/Jic mouse model of primary Sjorgren's syndrome. Autoimmunity 2003;36:247–54.

49 Tsunawaki S, Nakamura S, Ohyama Y *et al*. Possible function of salivary gland epithelial cells as non-professional antigen-presenting cells in the development of Sjogren's syndrome. J Rheumatol 2002;29:1884–96.

50 Mitsias DI, Tzioufas AG, Veiopoulou C *et al*. The Th1/Th2 cytokine balance changes with the progress of the immunopathological lesion of Sjogren's syndrome. Clin Exp Immunol 2002;128:562–8.

51 Cha S, Brayer J, Gao J *et al*. A dual role for interferon-gamma in the pathogenesis of Sjogren's syndrome-like autoimmune exocrinopathy in the nonobese diabetic mouse. Scand J Immunol 2004;60:552–65.

52 de Paiva CS, Villarreal AL, Corrales RM *et al*. Dry eye-induced conjunctival epithelial squamous metaplasia is modulated by interferon-{gamma}. Invest Ophthalmol Vis Sci 2007;48:2553–60.

53 Kullberg MC, Jankovic D, Feng CG *et al*. IL-23 plays a key role in *Helicobacter hepaticus*-induced T cell-dependent colitis. J Exp Med 2006;203:2485–94.

54 Khader SA, Bell GK, Pearl JE *et al*. IL-23 and IL-17 in the establishment of protective pulmonary CD4+ T cell responses after vaccination and during *Mycobacterium tuberculosis* challenge. Nat Immunol 2007;8:369–77.

55 Caspi RR, Chan CC, Grubbs BG *et al*. Endogenous systemic IFN-gamma has a protective role against ocular autoimmunity in mice. J Immunol 1994;152:890–9.

56 Dardalhon V, Korn T, Kuchroo VK, Anderson AC. Role of Th1 and Th17 cells in organ-specific autoimmunity. J Autoimmun 2008;31:252–6.